

Article

Synthesis, Structures and Properties of Cobalt Thiocyanate Coordination Compounds with 4-(hydroxymethyl)pyridine as Co-ligand

Stefan Suckert¹, Luzia S. Germann², Robert E. Dinnebier², Julia Werner¹ and Christian Näther^{1,*}

¹ Institut für Anorganische Chemie, Christian-Albrechts-Universität zu Kiel, Max-Eyth-Str. 2, Kiel 24118, Germany; ssuckert@ac.uni-kiel.de (S.S.); jwerner@ac.uni-kiel.de (J.W.)

² Max Planck Institut für Festkörperforschung, Heisenbergstr. 1, Stuttgart 70569, Germany; L.Germann@fkf.mpg.de (L.S.G.); R.Dinnebier@fkf.mpg.de (R.E.D.)

* Correspondence: cnaether@ac.uni-kiel.de; Tel.: +49-431-880-2092

Academic Editors: Thomas Doert and Mathias Wickleder

Received: 29 February 2016; Accepted: 24 March 2016; Published: 2 April 2016

Abstract: Reaction of $\text{Co}(\text{NCS})_2$ with 4-(hydroxymethyl)pyridine (hmpy) leads to the formation of six new coordination compounds with the composition $[\text{Co}(\text{NCS})_2(\text{hmpy})_4]$ (**1**), $[\text{Co}(\text{NCS})_2(\text{hmpy})_4] \times \text{H}_2\text{O}$ (**1-H₂O**), $[\text{Co}(\text{NCS})_2(\text{hmpy})_2(\text{EtOH})_2]$ (**2**), $[\text{Co}(\text{NCS})_2(\text{hmpy})_2(\text{H}_2\text{O})_2]$ (**3**), $[\text{Co}(\text{NCS})_2(\text{hmpy})_2]_n \cdot 4 \text{H}_2\text{O}$ (**4**) and $[\text{Co}(\text{NCS})_2(\text{hmpy})_2]_n$ (**5**). They were characterized by single crystal and powder X-ray diffraction experiments, thermal and elemental analysis, IR and magnetic measurements. Compound **1** and **1-H₂O** form discrete complexes, in which the Co(II) cations are octahedrally coordinated by two terminal thiocyanato anions and four 4-(hydroxymethyl)pyridine ligands. Discrete complexes were also observed for compounds **2** and **3** where two of the hmpy ligands were substituted by solvent, either water (**3**) or ethanol (**2**). In contrast, in compounds **4** and **5**, the Co(II) cations are linked into chains by bridging 4-(hydroxymethyl)pyridine ligands. The phase purity was checked with X-ray powder diffraction. Thermogravimetric measurements showed that compound **3** transforms into **5** upon heating, whereas the back transformation occurs upon resolution. Magnetic measurements did not show any magnetic exchange via the hmpy ligand for compound **5**.

Keywords: coordination compounds; thiocyanate; crystal structures; thermal properties; magnetic properties; Rietveld refinement

1. Introduction

The synthesis of new coordination polymers with desired physical properties is a major field in coordination chemistry [1–4]. For this purpose, structure–property relationships are investigated systematically and strategies for a rational construction of their crystal structures are required. Compounds that consist of paramagnetic metal cations are of particular interest because they can show different magnetic properties and thus it is not surprising that an increasing number of new compounds were recently reported [5–14]. One group of these compounds are transition metal thiocyanato coordination polymers, which show a variety of different coordination modes including the terminal and the bridging coordination, with the latter being of special importance because cooperative magnetic properties can be expected [15–34]. This is one reason why we are especially interested in thio- and selenocyanato coordination polymers, in which the metal centers are connected into chains by pairs of μ -1,3-bridging anionic ligands [35–47].

Metal thiocyanates with 4-(hydroxymethyl)pyridine (hmpy) are of particular interest as hmpy is known to act as terminal ligand, coordinating mainly *via* the pyridine N atom to the metal centers.

It is noted, that a few coordination compounds with this ligand were recently reported, which showed only coordination by the pyridine N atom except for two different metal complexes [48–53]. In the case of a copper(II)dipiconilate-4-(hydroxymethyl)pyridine coordination compound, the Cu(II) cations are linked by 4-(hydroxymethyl)pyridine ligands into chains, which was also observed in $\text{Ni}(\text{NCS})_2(4\text{-(hydroxymethyl)pyridine})_2$ [53,54].

Co(II) thiocyanate coordination compounds are of general interest because whenever Co(II) cations form polymeric chains with thiocyanato anions and are additionally coordinated by terminal N-bonded co-ligands, a slow relaxation of the magnetization might be observed, which can be traced back to the relaxation of single chains [44–47]. In this context, it is noted that for $[\text{Cd}(\text{N}_3)_2(4\text{-(hydroxymethyl)pyridine})_2]_n$ a crystal structure is found that is close to that of our desired compound [52]. In this compound, the Cd cations are linked by alternating μ -1,3 and μ -1,1 anionic azide anions into chains and are additionally coordinated by only N-bonded 4-(hydroxymethyl)pyridine ligands. However, a μ -1,1 coordination of the thiocyanate anions is very rare and therefore, for the desired compound, if it exists, one would expect alternating chains of only μ -1,3 bridging anionic ligands. Therefore, $\text{Co}(\text{NCS})_2$ was reacted in different molar ratios with 4-(hydroxymethyl)pyridine in several solvents. Five different coordination complexes were obtained, which were characterized by single crystal and X-ray powder diffraction (XRPD), thermal analysis, magnetic measurements and IR spectroscopy.

2. Results and Discussion

2.1. Synthetic Aspects

$\text{Co}(\text{NCS})_2$ mixed with 4-(hydroxymethyl)pyridine in different stoichiometric ratios in different solvents (e.g., water, methanol, ethanol and acetonitrile) formed five different crystalline materials. According to elemental and thermogravimetry (TG) analysis, the compositions of the compounds are $\text{Co}(\text{NCS})_2(\text{hmpy})_4$ (**1**), $\text{Co}(\text{NCS})_2(\text{hmpy})_4 \times \text{H}_2\text{O}$ (**1-H₂O**), $\text{Co}(\text{NCS})_2(\text{hmpy})_2(\text{EtOH})_2$ (**2**), $\text{Co}(\text{NCS})_2(\text{hmpy})_2(\text{H}_2\text{O})_2$ (**3**) and $\text{Co}(\text{NCS})_2(\text{hmpy})_2$ (**5**). Additionally, single crystals of a further compound of composition $\text{Co}(\text{NCS})_2(4\text{-(hmpy)})_2 \cdot 4 \text{H}_2\text{O}$ (**4**) were obtained.

2.2. Crystal Structures

2.2.1. $\text{Co}(\text{NCS})_2(4\text{-(hydroxymethyl)pyridine})_4$ (**1**) and $\text{Co}(\text{NCS})_2(4\text{-(hydroxymethyl)pyridine})_4 \times \text{H}_2\text{O}$ (**1-H₂O**)

Compound **1** crystallizes in the orthorhombic space group $P2_12_12_1$ with four formula units in the unit cell (Table 1). The asymmetric unit consists of one cobalt cation, two thiocyanate anions and four 4-(hydroxymethyl)pyridine ligands lying on general positions (Figure 1a and Figure S1 in the Supplementary Material). The CoN_6 octahedra are slightly distorted and the metal nitrogen distances are in the range of 2.099(3) to 2.179(2) Å and the angles are in the range of 88.06(9) to 92.66(9)° and from 176.27(9) to 178.42(10)° (Table S1 in the Supplementary Material). The discrete complexes are connected by intermolecular O-H...S hydrogen bonds between the H atom of the hydroxyl group and the thiocyanato S atom into layers that are parallel to the *ab* plane (Figure 1b and Table S2 in the Supplementary Material).

For compound **1-H₂O**, no single crystals were obtained. The powder pattern of this compound is similar to the one from the corresponding Ni compound, which was recently reported [53]. Rietveld analysis of **1-H₂O** (see Experimental Section, Table 1 and Figure S2 in the Supplementary Material) confirmed that both complexes are isostructural. **1-H₂O** crystallizes in the cubic space group $Pn\bar{3}n$ with six formula units in the unit cell. The crystal structure consists, similar to compound **1**, of discrete complexes, in which the Co(II) cations are coordinated by two N-bonded thiocyanate anions and four 4-hydroxypyridine ligands in an octahedral fashion (Figure S3 in the Supplementary Material). The crystal packing led to the formation of voids in which additional water is embedded. **1-H₂O** contains roughly 2 water molecules per sum formula, determined from XRPD. The water shows

a similar disorder as in the isostructural Ni-complex (two orientations, both on special positions, threefold rotoinversion and three-fold axis, respectively). The presence of water was confirmed by thermogravimetric analysis.

Table 1. Selected crystal data and details on the structure determinations for compounds 1, 2, 3 and 4.

Compound	1	2	3	4
Formula	$C_{26}H_{28}CoN_6O_4S_2$	$C_{18}H_{26}CoN_4O_4S_2$	$C_{14}H_{18}CoN_4O_4S_2$	$C_{14}H_{22}CoN_4O_6S_2$
MW/g mol ⁻¹	611.59	485.48	429.37	465.40
crystal system	<i>orthorhombic</i>	<i>monoclinic</i>	<i>orthorhombic</i>	<i>triclinic</i>
space group	$P2_12_12_1$	$C2/c$	$Pbca$	$P\bar{1}$
<i>a</i> /Å	11.5440(3)	9.0056(4)	12.3007(5)	7.3858(7)
<i>b</i> /Å	14.3213(3)	16.1092(7)	7.7432(5)	7.6952(6)
<i>c</i> /Å	17.6437(4)	16.3412(8)	19.3263(14)	9.4172(9)
β /°	90	95.446(4)	90	70.828(10)
<i>V</i> /Å ³	2916.95(12)	2359.97(19)	1840.77(16)	491.53(8)
<i>T</i> /K	200(2)	200(2)	200(2)	200(2)
<i>Z</i>	4	4	4	1
D_{calc} /mg·cm ⁻³	1.393	1.366	1.549	1.572
μ /mm ⁻¹	0.773	0.933	1.1185	1.123
θ_{max} /deg	1.83 to 27.96	2.53 to 27.51	2.11 to 27.94	2.35 to 27.91
measured refl.	31835	11473	13046	5125
unique refl.	6972	2700	2190	2277
Refl. ($F_0 > 4\sigma(F_0)$)	6397	2299	1808	1952
parameter	356	151	116	126
R_{int}	0.0525	0.0402	0.0441	0.0335
R_1 ($F_0 > 4\sigma(F_0)$)	0.0343	0.0514	0.0473	0.0406
wR_2 (all data)	0.0708	0.1217	0.1134	0.1115
GOF	1.106	1.074	1.132	1.043
$\Delta\rho_{max/min}$ /e Å ⁻³	0.276/−0.322	0.710/−0.803	0.475/−0.527	0.541/−0.555

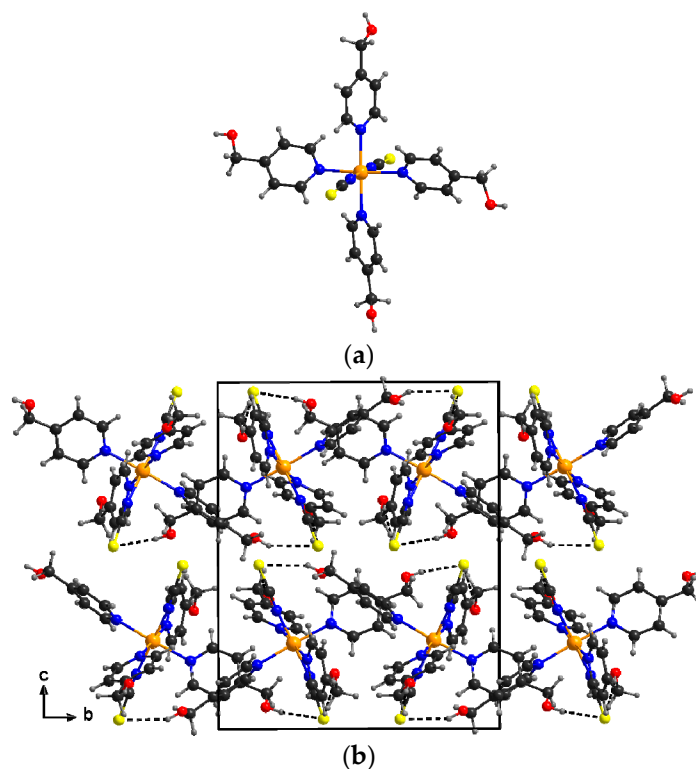


Figure 1. Crystal structure of 1 with view of the coordination sphere (a) and along the crystallographic *a* axis with intermolecular hydrogen bonding shown as dashed lines (b). The ORTEP plot is shown in Figure S1 in the Supplementary Material.

2.2.2. $\text{Co}(\text{NCS})_2(4\text{-(hydroxymethyl)pyridine})_2(\text{EtOH})_2$ (**2**) and $\text{Co}(\text{NCS})_2(4\text{-(hydroxymethyl)pyridine})_2(\text{H}_2\text{O})_2$ (**3**)

Compounds **2** and **3** form simple solvate complexes, in which the Co(II) cations are coordinated by two terminally bonded thiocyanate anions, two terminally bonded 4-(hydroxymethyl)pyridine ligands, and two ethanol, respectively, water molecules with a slightly distorted octahedral coordination geometry (Figure 2, Figures S4 and S5 in the Supplementary Material).

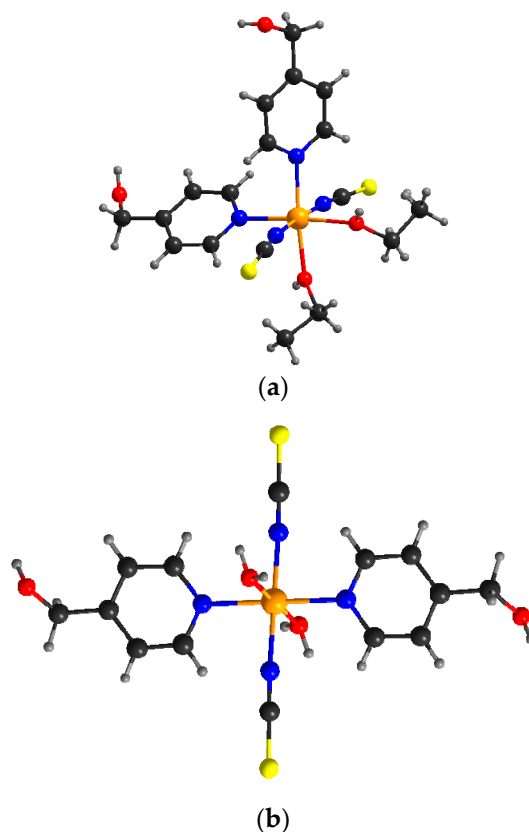


Figure 2. View of the discrete complexes in the crystal structure of **2** (a) and **3** (b), showing the coordination sphere of the Co(II) cations. ORTEP plots of **2** and **3** can be found in Figures S4 and S5 in the Supplementary Material.

Compound **2** crystallizes in the monoclinic space group $C2/c$ with four formula units in the unit cell. The Co(II) cations are located on two-fold rotation axes, whereas complex **3** crystallizes in the orthorhombic space group $Pbca$ with $Z = 4$ and the cobalt cations located on inversion centers (Table 1).

Although compounds **2** and **3** show a six-fold coordination of the cations, the coordination is different: In compound **2** the anionic ligands are *trans* coordinated, whereas the N-donor co-ligands and the ethanol molecules are *cis* coordinated (Figure 2a). In contrast, in compound **3** all ligands are *trans* coordinated, which is somewhat surprising because the ethanol molecules might occupy more space than water molecules (Figure 3b). The cobalt nitrogen distances in compound **2** are in the range of 2.078(3) to 2.158(2) Å while the cobalt oxygen distances are around 2.078(3) Å with angles ranging from 86.26(12) to 91.90(10)° and from 175.51(9) to 176.8(10)° (Table S3 in the Supplementary Material). For compound **3**, the cobalt nitrogen distances are in the range of 2.085(3) Å to 2.180(3) Å and the cobalt oxygen distances are 2.101(2) Å with bonding angles in the range of 86.80(10) to 91.20(10)° and of 180 (Table S3 in the Supplementary Material).

In compound **2** the discrete complexes are connected by intermolecular O–H...S hydrogen bonding between the H atom of the methanol group of the 4-(hydroxymethyl)pyridine ligand and

the thiocyanato S atom of a neighbored complex into chains along the crystallographic *b* axis. These chains are further connected into layers by intermolecular O–H···O hydrogen bonding between the hydroxyl H atom of the ethanol molecules of one complex and the hydroxyl O atom of a neighboring complex (Figure 3a and Table S4 in the Supplementary Material).

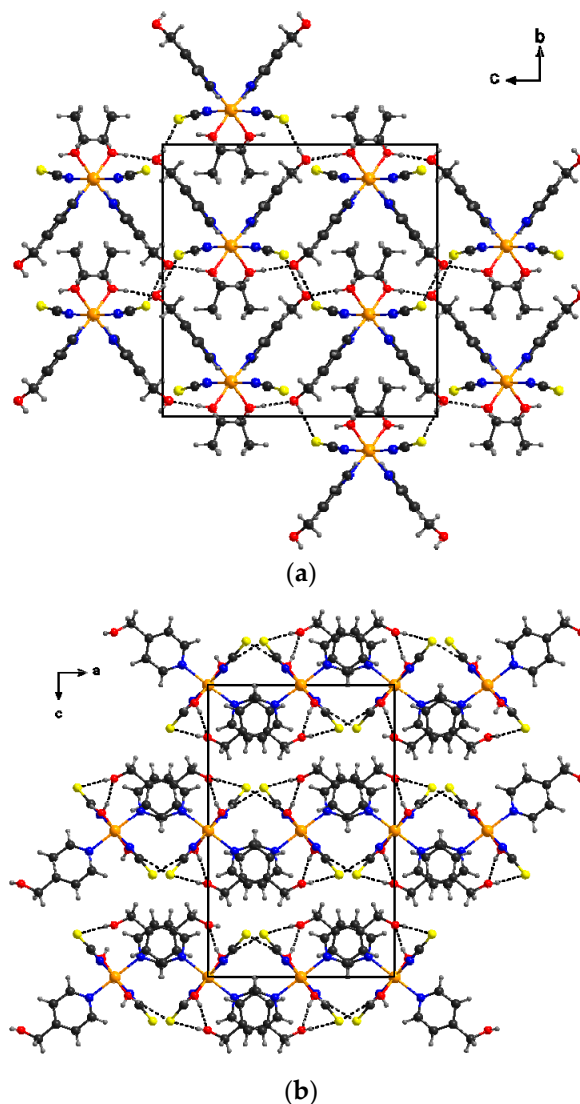


Figure 3. Crystal structure of **2** with view along the crystallographic *b* axis (a) and of **3** with view along the crystallographic *b* axis (b). Intermolecular hydrogen bonding is shown as dashed lines.

In compound **3**, the complexes are connected by intermolecular O–H···O hydrogen bonding between the methanol group of the 4-(hydroxymethyl)pyridine ligand and the water molecule into chains, that are further linked into layers by additional intermolecular O–H···S hydrogen bonding between the H atoms of the water molecules and the thiocyanate S atoms of neighbored complexes (Figure 3: bottom and Table S4 in the Supplementary Material).

2.2.3. [Co(NCS)₂(4-(hydroxymethyl)pyridine)₂]_n·4 H₂O (**4**)

Compound **4** crystallizes in the triclinic space group $P\bar{1}$ with 1 formula unit in the unit cell (Table 1). The Co(II) cation lies on a special position and is octahedrally coordinated by four μ -1,6 bridging 4-(hydroxymethyl)pyridine ligands and two terminally N bonded thiocyanate anions (Figure 4a and Figure S6 in the Supplementary Material). The cobalt nitrogen distances are in the range of 2.078(2)

to 2.1603(18) Å and the cobalt oxygen distances amount to 2.1412(15) Å with bonding angles in the range of 88.18(7) to 91.82(7)° and 180° (Table S5 in the Supplementary Material). The crystal structure consists of four water molecules per sum formula, located between the 1D polymers (Figure 4).

The Co(II) cations are linked by pairs of the 4-(hydroxymethyl)pyridine ligands into chains that elongate in the direction of the crystallographic *a* axis (Figure 4a). These chains are further linked via hydrogen bonding to the solvate water molecules. Intermolecular O–H···S hydrogen bonds are observed between H atoms from water molecules or from the hydroxyl group of the 4-(hydroxymethyl)pyridine ligand and the thiocyanate S atoms of neighboring chains (Figure 4b). The water molecules are also linked to the hydroxyl group by intermolecular O–H···O hydrogen bonding (Figure 4b and Table S6 in the Supplementary Material).

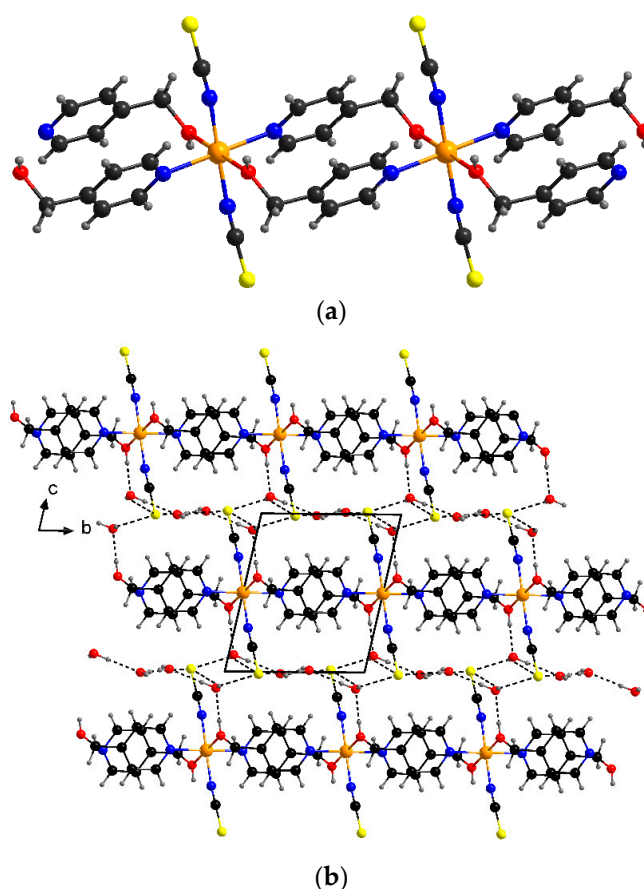


Figure 4. Crystal structure of 4 with view of the chain (a) and with view along the crystallographic *a* axis (b). Intermolecular hydrogen bonding shown as dashed lines and an ORTEP plot is shown in Figure S6 in the Supplementary Material.

2.2.4. [Co(NCS)₂(4-(hydroxymethyl)pyridine)₂]_n (5)

No single crystals were obtained for compound 5. Its crystal structure was determined from XRPD data by refining the recently reported, isostructural Ni-complex (see Experimental Section, Table 1 and Figure S7 in the Supplementary Material) [53]. [Co(NCS)₂(hmpy)₂] crystallizes in the monoclinic space group *P*2₁/*c* with four formula units in the unit cell and all atoms lying on general positions. The Co(II) cations are coordinated by one terminal and two bridging thiocyanate anions groups as well as one terminal and two bridging 4-(hydroxymethyl)pyridine ligands and show a slightly distorted octahedral coordination geometry (Figure 5). Half of the thiocyanate anions are connecting two neighboring cobalt ions, which are further connected by the ligand hmpy to form a zig zag polymer along the [100] direction.

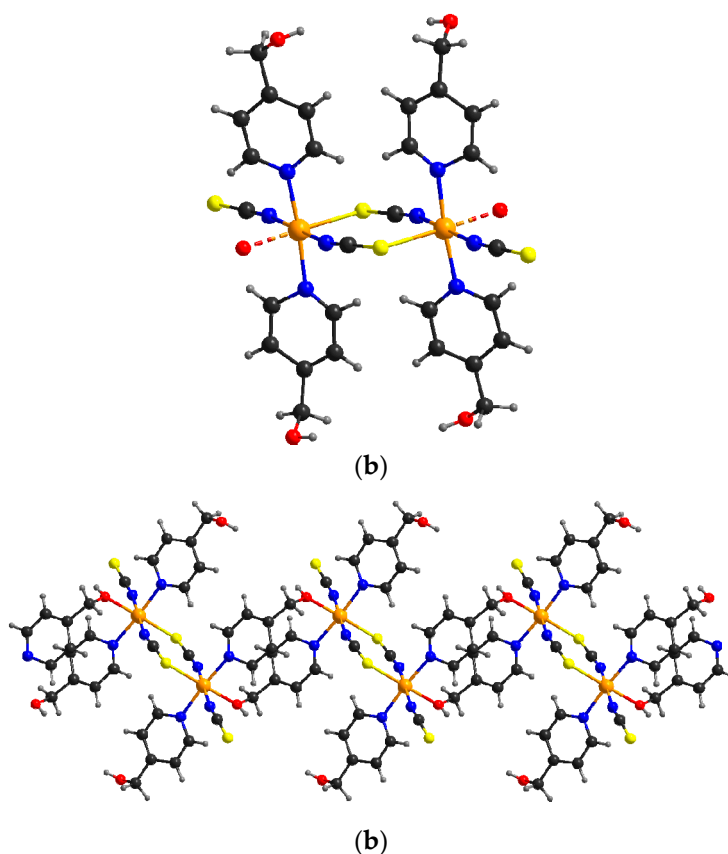


Figure 5. Crystal structure of 5 with view of the dimer (a) and the chain (b).

Based on the crystal structure, X-ray powder patterns were calculated and compared with the experimental pattern. Careful inspection of the measured powder pattern revealed that most of the compounds were obtained as pure phase, except for some batches of compounds 2 and 4 (Figures S8–S13 in the Supplementary Material). In both cases, some additional, weak reflections appeared in the measured pattern, indicating not further characterized impurities. This is not really surprising because so many related compounds were obtained, so it is assumed that they exist in equilibrium in solution. Moreover, compound 4 was found to be quite unstable and easily loses the water molecules. This is also the case for the ethanol solvate 2 which loses some of the solvent even at room-temperature.

2.3. IR Spectroscopy

All compounds were measured by IR-spectroscopy, to investigate if the coordination mode of the anionic ligands can be determined from the value of the asymmetric CN stretching vibration. Usually for compounds with terminally N-bonded thiocyanato anions a value below 2100 cm^{-1} is expected, whereas for μ -1,3 bridging thiocyanato anions this vibration should be observed above 2100 cm^{-1} [38]. It is noted that for some compounds these regions overlap and a definite decision cannot be made. This is especially the case for discrete complexes with terminally N-bonded anionic ligands, where the metal centers are additionally coordinated by O-donor ligands like, e.g., water. In this case this value is usually shifted to higher wavenumbers [30].

However, for compounds 1 and 1-H₂O the value of the CN stretching vibration is observed at 2073 cm^{-1} and $2084/2095\text{ cm}^{-1}$ indicating an N-terminal coordination of the thiocyanato anions, which is in agreement with the crystal structure (Figures S14 and S15 in the Supplementary Material). For the solvate complexes 2 and 3, the CN stretching vibration is observed at 2090 and 2115 cm^{-1} and at 2098 and 2111 cm^{-1} , which is at the border line between the values expected for terminal and

bridging NCS ligands (Figures S16 and S17 in the Supplementary Material). However, as mentioned above they are shifted to higher values, because in both compounds the Co(II) cations are additionally coordinated by oxygen atoms from the hydroxyl group. For compound **4**, the CN vibration occurs at 2092 cm^{-1} , which is reasonable because the cations are coordinated by terminal anions and only N-bonded 4-(hydroxymethyl)pyridine ligands (Figure S18 in the Supplementary Material). Finally, for compound **5**, the CN vibrations are found at 2115 , 2092 and 2098 cm^{-1} , which again is consistent with the results of the structure determination showing both terminal and bridging NCS ligands (Figure S19 in the Supplementary Material).

It is noted that all five compounds show very broad bands above 3000 cm^{-1} , which belong to the O-H stretching-vibration of the hmpy ligand.

2.4. Thermoanalytical Measurements

To investigate the thermal properties of the compounds, measurements using simultaneously differential thermoanalysis and thermogravimetry (DTA-TG) were performed. In this context it was checked if a different, e.g., metastable modification of $[\text{Co}(\text{NCS})_2(4\text{-(hydroxymethyl)pyridine})_2]_n$ can be obtained as recently reported for other ligands [22,24,30].

Compound **1** shows two very poorly resolved mass steps in the TG curve upon heating, which are accompanied by endothermic signals in the DTA curve (Figure 6 and Figure S20 in the Supplementary Material). The experimental mass loss of the first TG step ($\Delta m_{\text{exp}} = 39\%$) is in reasonable agreement with the calculated mass loss assuming the loss of two 4-(hydroxymethyl)pyridine ligands ($\Delta m_{\text{calc}} = 36\%$). The thermogravimetric curve of **1-H₂O** looks similar, except that a further mass loss is observed at lower temperatures, which is associated with the removal of water molecules, which are located in the crystal cavities (Figure 6 and Figure S20 in the Supplementary Material). In order to check whether the water removal leads to compound **1**, as it was recently reported for the isostructural Ni-complex [53], the measurement was repeated and interrupted after the first mass loss. XRPD investigations showed, that a phase of poor crystallinity was obtained, which could neither be identified nor indexed.

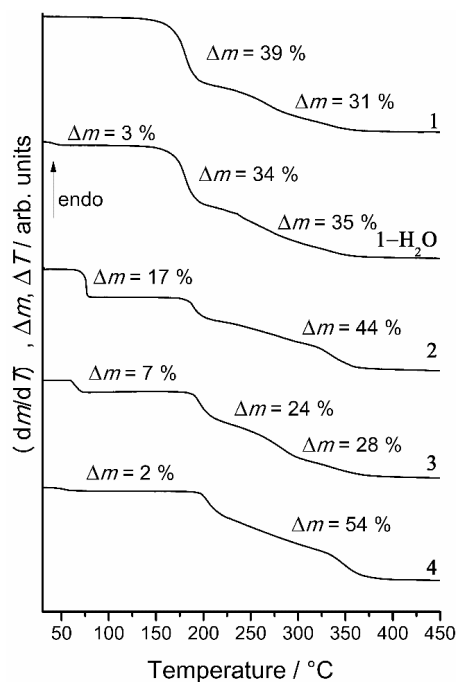


Figure 6. Thermogravimetric curves for compounds **1**, **1-H₂O**, **2**, **3** and **4**. Heating rate = $1\text{ }^{\circ}\text{C}/\text{min}$ (**1**, **1-H₂O**, **2**), and heating rate = $4\text{ }^{\circ}\text{C}/\text{min}$ (**3**, **4**). Given is the mass loss in %.

TG measurements of compound **2** and **3** showed a subsequent mass loss. The first step was associated with a desolvation process ($\Delta m_{(\text{calc})} = 19\%$ for **2** and 8.4% for **3**) (Figure 6 and Figure S21 in the Supplementary Material). The calculated and measured Δm for compound **4** deviates, which was attributed to its instability and therefore partial desolvation upon storage (Figure 6 and Figure S22 in the Supplementary Material).

To identify the intermediates, which were formed by removal of the 4-(hydroxymethyl)pyridine ligand respectively water or ethanol, the TG measurements were repeated and stopped after the corresponding steps and the isolated residues were investigated by XRPD (Figure 7).

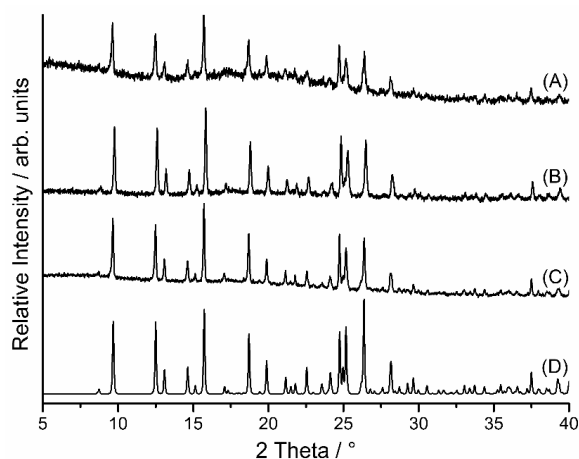


Figure 7. Experimental XRPD patterns of the residue obtained from **4** (A); **3** (B) and from **2** (C) and calculated XRPD pattern of compound **5** (D).

The residue of **1** is amorphous, observed by XRPD data, while compounds **2**, **3** and **4** transformed into $[\text{Co}(\text{NCS})_2(4\text{-(hydroxymethyl)pyridine})_2]_n$ (**5**), which was obtained as a pure phase (Figure 7). It is noted that after removal of all ligands in several cases good crystalline powders are observed that consists of $\text{Co}(\text{NCS})_2$.

2.5. Resolution

To investigate if compound **1** can be transformed into **1-H₂O**, a saturated solution of **1** with an excess of solid was stirred in water and the residue was investigated by XRPD (Figure 8). Comparison of the measured powder pattern proofed that **1** completely transforms into **1-H₂O**.

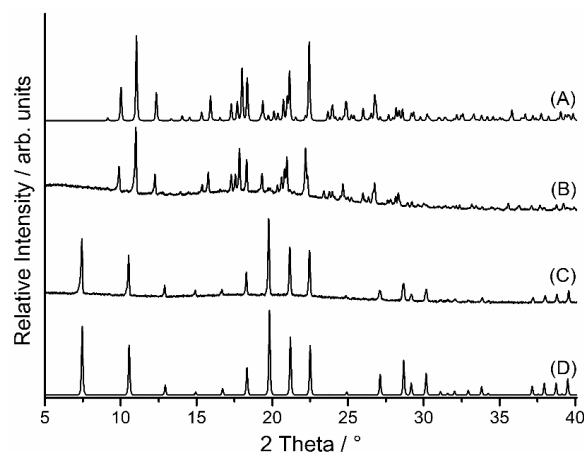


Figure 8. Calculated XRPD patterns of **1** (A) and **1-H₂O** (D). The experimental XRPD patterns of **1** (B); and of the product obtained after stirring this compound in water for 2 d (C).

In additional experiments, compound **5** was soaked either in water or ethanol and the compounds were investigated by XRPD afterwards. Compound **5** can transform into the hydrated form **3**, after soaking in water for three days (Figure 9), whereas no transformation was observed after the treatment in ethanol. No transformation of compound **5** takes place while kept in an aqueous or EtOH atmosphere for several days.

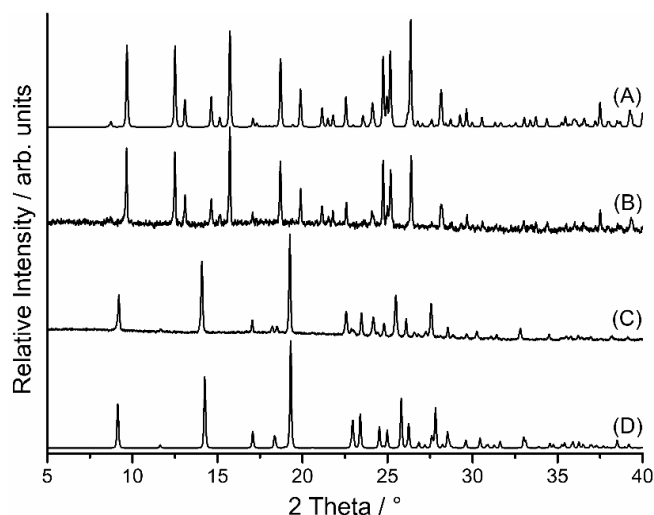


Figure 9. Calculated XRPD patterns of **5** (A) and **3** (D). The experimental XRPD patterns of the residue obtained after the first mass step (B); and of the product obtained after stirring compound **5** in water for 3 d (C).

2.6. Magnetic Investigations

For compound **5**, the temperature dependence of the susceptibility was measured at $H_{DC} = 1000$ Oe. The χ_M versus T curve shows a steady increase with decreasing temperature, which indicates only paramagnetic behavior (Figure 10).

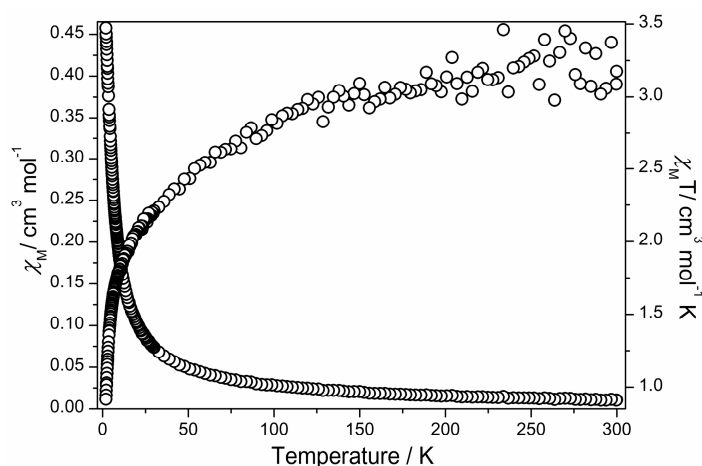


Figure 10. χ_M and $\chi_M T$ as a function of the temperature for **5** at $H_{DC} = 1000$ Oe.

The $\chi_M T$ value decreases on cooling, which is indicative for dominating antiferromagnetic interactions (Figure 10). The analysis of the magnetic data according to the Curie–Weiss law results in a negative Weiss constant of $\theta = -18.85$ K and is therefore in agreement with the antiferromagnetic interactions. Calculations of the Curie constant yielded a value of $3.37 \text{ cm}^3 \cdot \text{K} \cdot \text{mol}^{-1}$, from which an experimental effective magnetic moment of $5.19 \mu_B$ was calculated. This value is slightly higher than

the theoretical value of $3.87 \mu_B$ for Co^{2+} in a high spin configuration and this can be traced back to the strong spin-orbit coupling for Co(II). AC measurements show a steady increase of the susceptibility in χ_M' and no signal in χ_M'' as expected for only paramagnetic behavior and this behavior is also indicated by field dependent magnetic measurements (Figures S23 and S24 in the Supplementary Material). Therefore, this ligand does not mediate strong magnetic exchange, but it cannot be excluded that some magnetic order is observed at very low temperatures.

3. Experimental Section

3.1. General

4-(hydroxymethyl)pyridine and $\text{Co}(\text{NCS})_2$ were obtained from Alfa Aesar (Ward Hill, MA, USA). All chemicals and solvents were used without further purification. Crystalline powders of all compounds were prepared by stirring the reactants in the respective solvents at room temperature. The residues were filtered and washed with appropriate solvents and dried in air. The purity of all compounds was checked by XRPD and elemental analysis.

3.2. Synthesis of Compound 1

Single crystals suitable for single crystal X-ray diffraction were prepared by the reaction of $\text{Co}(\text{NCS})_2$ (26.3 mg, 0.15 mmol) and 4-(hydroxymethyl)pyridine (65.5 mg, 0.60 mmol) in 1.5 mL acetonitrile at room temperature for 1 d. A crystalline powder was synthesized by stirring $\text{Co}(\text{NCS})_2$ (87.6 mg, 0.50 mmol) and 4-(hydroxymethyl)pyridine (218.6 mg, 2.0 mmol) in 1.5 mL acetonitrile for 2 d. Yield: 75% elemental analysis calc. (%) for $\text{C}_{26}\text{H}_{28}\text{CoN}_6\text{O}_4\text{S}_2$: C 51.06, H 4.61, N 13.74; S 10.49; found C 50.4, H 4.49, N 13.25, S 9.90. IR (ATR): ν_{max} = 3410 (b), 3056 (w), 2884(w), 2806 (w), 2082 (s), 1613 (s), 1562 (m), 1504 (s), 1561 (m), 1453 (w), 1420 (s), 1337 (m), 1221 (s), 1100 (m), 1046 (s), 1016 (s), 804 (s), 726 (m), 603 (m), 486 (m).

3.3. Synthesis of Compound 1-H₂O

A crystalline powder was synthesized by stirring $\text{Co}(\text{NCS})_2$ (87.6 mg, 0.50 mmol) and 4-(hydroxymethyl)pyridine (272.8 mg, 2.50 mmol) at room temperature in 3 mL water for 1 d. Yield: 82% elemental analysis calc. (%) for $\text{C}_{26}\text{H}_{30}\text{CoN}_6\text{O}_5\text{S}_2$: C 49.60, H 4.80, N 13.35; S 10.19; found C 48.57, H 4.87, N 12.69, S 9.67. IR (ATR): ν_{max} = 3405 (b), 3065 (w), 2865(w), 2805 (w), 2071 (s), 1613 (s), 1561 (m), 1503 (w), 1451 (w), 1422 (s), 1337 (m), 1221 (s), 1099 (m), 1049 (s), 1016 (s), 805 (s), 724 (m), 603 (m), 482 (s).

3.4. Synthesis of Compound 2

Single crystals suitable for single crystal X-ray diffraction were prepared by the reaction of $\text{Co}(\text{NCS})_2$ (26.3 mg, 0.15 mmol) 4-(hydroxymethyl)pyridine (32.7 mg, 0.30 mmol) at room temperature in 1.5 mL ethanol. A crystalline powder was synthesized by stirring $\text{Co}(\text{NCS})_2$ (175.1 mg, 1.00 mmol) and 4-(hydroxymethyl)pyridine (109 mg, 1.00 mmol) at room temperature in 3 mL ethanol for 1 d. Yield: 62% elemental analysis calcd (%) for $\text{C}_{18}\text{H}_{26}\text{CoN}_4\text{O}_4\text{S}_2$: C 44.53, H 5.40, N 11.54; S 13.21; found C 38.25, H 3.26, N 12.70, S 16.58. IR (ATR): ν_{max} = 3250 (b), 3075 (w), 2980 (w), 2885(w), 2090 (s), 1613 (s), 1559 (m), 1506 (w), 1420 (s), 1375 (m), 1320 (w), 1221 (m), 1092 (m), 1046 (m), 1018 (s), 984 (m), 882 (w), 798 (s), 720 (w), 666 (s), 604 (s), 481 (s).

3.5. Synthesis of Compound 3

Single crystals suitable for single crystal X-ray diffraction were prepared by the reaction of $\text{Co}(\text{NCS})_2$ (26.3 mg, 0.15 mmol) 4-(hydroxymethyl)pyridine (65.5 mg, 0.60 mmol) at room temperature in 1.5 mL water. A crystalline powder was synthesized by stirring $\text{Co}(\text{NCS})_2$ (175.1 mg, 1.00 mmol) and 4-(hydroxymethyl)pyridine (109 mg, 1.00 mmol) at room temperature in 1 mL water for 5 d. Yield: 72% elemental analysis calcd (%) for $\text{C}_{14}\text{H}_{18}\text{CoN}_4\text{O}_4\text{S}_2$: C 39.16, H 4.23, N 13.05; S 14.94; found C 39.03, H

4.16, N 13.62, S 14.77. IR (ATR): ν_{\max} = 3314 (b), 2889(w), 2862 (w), 2111 (s), 2098 (s), 1647 (m), 1614 (m), 1562 (m), 1503 (w), 1450 (w), 1422 (s), 1389 (w), 1358 (w), 1361 (w), 1225 (m), 1103 (m), 1036 (s), 1016 (s), 981 (m), 807 (s), 610 (s), 466 (s).

3.6. Synthesis of Compound 4

Single crystals suitable for single crystal X-ray diffraction were prepared by the reaction of $\text{Co}(\text{NCS})_2$ (26.3 mg, 0.15 mmol) and 4-(hydroxymethyl)pyridine (37.7 mg, 0.30 mmol) in 1.5 mL water at 105 °C in a closed glass culture tube. A crystalline powder was synthesized by stirring $\text{Co}(\text{NCS})_2$ (26.3 mg, 0.15 mmol) and 4-(hydroxymethyl)pyridine (32.7 mg, 0.30 mmol) at room temperature in 1.5 mL water for 3 d. Yield: 80% elemental analysis calcd (%) for $\text{C}_{14}\text{H}_{22}\text{CoN}_4\text{O}_6\text{S}_2$: C 36.13, H 4.76, N 12.04; S 13.78; found C 35.93, H 4.00, N 11.73, S 13.72. IR (ATR): ν_{\max} = 3507 (b), 3445 (b), 3353 (b), 3144 (b), 2976 (w), 2937 (w), 2842 (w), 2092 (s), 1615 (m), 1564 (m), 1446 (w), 1422 (s), 1371 (w), 1221 (m), 1107 (w), 1069 (w), 1007 (s), 855 (s), 808 (s), 744 (w), 608 (s), 512 (s).

3.7. Synthesis of Compound 5

A crystalline powder was synthesized by stirring $\text{Co}(\text{NCS})_2$ (87.6 mg, 0.50 mmol) and 4-(hydroxymethyl)pyridine (109.1 mg, 1.00 mmol) in 3.0 mL water for 5 d. Yield: 74% elemental analysis calcd (%) for $\text{C}_{14}\text{H}_{14}\text{CoN}_4\text{O}_2\text{S}_2$: C 42.75, H 3.59, N 14.24; S 16.30; found C 42.00, H 3.46, N 14.35, S 15.04. IR (ATR): ν_{\max} = 3426 (b), 3235 (b), 2886 (w), 2115 (s), 2098 (s), 2092 (s), 1615 (m), 1561 (w), 1504 (w), 1422 (s), 1391 (m), 1369 (m), 1324 (w), 1225 (m), 1198 (m), 1100 (w), 1039 (m), 1016 (s), 970 (m), 849 (s), 801 (s), 723 (w), 607 (s), 507 (m).

3.8. Elemental Analysis

CHNS analysis was performed using a EURO EA elemental analyzer, fabricated by EURO VECTOR Instruments and Software.

3.9. IR Spectroscopy

The IR spectra were measured using an ATI Mattson Genesis Series FTIR Spectrometer, control software: WINFIRST, from ATI Mattson (Midland, ON, Canada).

3.10. Differential Thermal Analysis and Thermogravimetry

The heating-rate dependent DTA-TG measurements were performed in a nitrogen atmosphere (purity: 5.0) in Al_2O_3 crucibles using a STA-409CD instrument from Netzsch (Exton, PA, USA). All measurements were performed with a flow rate of $75 \text{ mL} \cdot \text{min}^{-1}$ and were corrected for buoyancy and current effects. The instrument was calibrated using standard reference materials.

3.11. Single-Crystal Structure Analysis

Single-crystal data collections were performed on an imaging plate diffraction system: Stoe IPDS-1 for **4** as well as Stoe IPDS-2 for **2**, **3** with $\text{MoK}\alpha$ radiation. The structures were solved with Direct Methods using SHELXS-97 and structure refinements were performed using least-squares methods against F^2 using SHELXL-2013. [55] Numerical absorption corrections were applied using X-RED and X-SHAPE of the program package X-Area. All non-hydrogen atoms were refined with anisotropic thermal displacement parameters. All hydrogen atoms were positioned with idealized geometry and were refined isotropic with an $U_{\text{iso}}(\text{H}) = -1.2 U_{\text{eq}}(\text{C})$ (1.5 for methyl H atoms) of the corresponding parent atom using a riding model. The hydroxyl hydrogen atoms were located in the difference Fourier map, their bond lengths were set to ideal values and finally they were refined using a riding model. The disorder of the ethyl group in compound **2** was modeled using a split model. CCDC 1455775 (**1**), CCDC 1455776 (**1-H₂O**), CCDC 1455777 (**2**), CCDC 1455778 (**3**), CCDC 1455779 (**4**) and CCDC 1455780

(5) contain the supplementary crystallographic data for this paper. These data can be obtained free of charge via <http://www.ccdc.cam.ac.uk/conts/retrieving.html>.

3.12. X-Ray Powder Diffraction

The measurements were performed using: (1) a PANalytical X'Pert Pro MPD Reflection Powder Diffraction System with $\text{CuK}\alpha_1$ radiation ($\lambda = 1.540598 \text{ \AA}$) equipped with a PIXcel semiconductor detector from PANalytical; (2) a Stoe Transmission Powder Diffraction System (STADI P) with $\text{CuK}\alpha_1$ radiation ($\lambda = 1.540598 \text{ \AA}$) equipped with a MYTHEN 1K1 detector and a Johansson-type Ge(111) monochromator from STOE & CIE; and (3) a Stoe Stadi-P machine ($\text{Mo K}\alpha$ radiation, $\lambda = 0.7093 \text{ \AA}$), equipped with a MYTHEN 1K detector and a Johansson-type Ge(111) monochromator in Debye Scherrer mode. Rietveld refinements [56] of **1-H₂O** and **5** were performed using TOPAS 5.0. [57]. Structure determination of compounds **1-H₂O** and **5** was performed by Rietveld refinements of the corresponding isostructural Ni-complexes (Table 2). The profile function was described in both cases with the fundamental parameter approach [55], while the background was modelled by Chebyshev polynomials of 12th and 11th order. The Rietveld refinement for compound **5** was carried out using a rigid body model for describing the ligand hmpy, whereas the individual bond lengths of the thiocyanate group were restrained. For both compound **1-H₂O** and **5**, hydrogen atoms were fixed at geometric calculated positions and an overall isotropic thermal displacement parameter was used for all atoms.

Table 2. Selected crystal data and details of the Rietveld refinements for compounds **1-H₂O** and **5**.

Compound	1-H₂O	5
formula	$\text{C}_{26}\text{H}_{31.4}\text{CoN}_6\text{O}_{5.7}\text{S}_2$	$\text{C}_{14}\text{H}_{14}\text{CoN}_4\text{O}_2\text{S}_2$
MW/g mol ⁻¹	641.83	393.35
Crystal system	cubic	monoclinic
Space group	$Pn\bar{3}n:2$	$P2_1/c$
$a/\text{\AA}$	16.7494(6)	10.7088(6)
$b/\text{\AA}$	16.7494(6)	20.2164(11)
$c/\text{\AA}$	16.7494(6)	7.9016(4)
$\alpha/^\circ$	90	90
$\beta/^\circ$	90	107.181(3)
$\gamma/^\circ$	90	90
$V/\text{\AA}^3$	4698.9(5)	1634.32(15)
T/K	293 (2)	293 (2)
Z	6	4
$D_{\text{calc}}/\text{mg}\cdot\text{cm}^{-3}$	1.355	1.599
μ/mm^{-1}	0.7468	1.35197
$\lambda/\text{\AA}$	0.7093	0.7093
$\theta_{\text{max}}/\text{deg}$	2.00 to 49.80	2 to 49.80
$R_{\text{wp}}/\% \text{ }^a$	5.54	4.84
$R_{\text{p}}/\% \text{ }^a$	4.33	3.66
$R_{\text{exp}}/\% \text{ }^a$	1.76	1.67
$R_{\text{Bragg}}/\% \text{ }^a$	4.01	2.89

Note: ^a as defined in TOPAS [56].

3.13. Magnetic Measurements

All magnetic measurements were performed using a PPMS (Physical Property Measurement System) from Quantum Design, which was equipped with a 9 Tesla magnet. The data were corrected for core diamagnetism.

4. Conclusions

In the present contribution, investigations on new cobalt(II) thiocyanato coordination compounds with 4-(hydroxymethyl)pyridine as ligand are reported, with the major goal to prepare a 1D compound in which the Co(II) cations are linked by the anionic ligands into chains. Even if several new compounds were discovered and analyzed with single crystal and powder X-ray diffraction, thermal and elemental analysis, magnetic and IR measurements, most of them consist of simple discrete complexes that are coordinated in part by additional solvent molecules. One of these compounds (**5**) exhibits a composition that corresponds to that, expected for the desired compound but unfortunately, its crystal structure consists of only Co(NCS)₂ dimers that are linked into chains by the 4-(hydroxymethyl)pyridine ligand. Some of these compounds can be thermally decomposed, which either leads to amorphous products or to the formation of **5**. There is no indication for the formation of a further modification with the desired structural features, even if a similar structure is known for the corresponding azido compound with Cd(II) as cation.

Supplementary Materials: The supplementary materials are available online at www.mdpi.com/2073-4352/6/4/38/s1. IR spectra, DTA-TG curves, experimental and calculated X-ray powder patterns as well as tables with selected bond lengths and angles.

Acknowledgments: This project was supported by the Deutsche Forschungsgemeinschaft (Project No. NA 720/5-1) and by the State of Schleswig-Holstein. We thank Wolfgang Bensch for access to his experimental facilities. Special thanks to Maren Rasmussen and Henning Lühmann for the magnetic measurements.

Author Contributions: Stefan Suckert and Julia Werner were responsible for the synthesis and the analytical characterization of all compounds. Luzia S. Germann and Robert E. Dinnebier performed the structure determinations from X-ray powder diffraction data and Christian Näther was responsible for part of the single crystal structure determinations. All authors were involved in the writing process of this manuscript.

Conflicts of Interest: The authors declare no conflict of interest.

References

1. Diaz-Torres, R.; Alvarez, S. Coordinating ability of anions and solvents towards transition metals and lanthanides. *Dalton Trans.* **2011**, *40*, 10742–10750. [[CrossRef](#)] [[PubMed](#)]
2. Batten Stuart, R.; Champness Neil, R.; Chen, X.-M.; Garcia-Martinez, J.; Kitagawa, S.; Öhrström, L.; O’Keeffe, M.; Paik Suh, M.; Reedijk, J. Terminology of metal-organic frameworks and coordination polymers (iupac recommendations 2013). *Pure Appl. Chem.* **2013**, *85*, 1715–1724.
3. Janiak, C.; Vieth, J.K. Mofs, mils and more: Concepts, properties and applications for porous coordination networks (PCNs). *New J. Chem.* **2010**, *34*, 2366–2388. [[CrossRef](#)]
4. Aakeroy, C.B.; Champness, N.R.; Janiak, C. Recent advances in crystal engineering. *CrystEngComm* **2010**, *12*, 22–43. [[CrossRef](#)]
5. Miller, J.S.; Gatteschi, D. Molecule-based magnets. *Chem. Soc. Rev.* **2011**, *40*, 3065–3066. [[CrossRef](#)] [[PubMed](#)]
6. Wang, X.Y.; Avendano, C.; Dunbar, K.R. Molecular magnetic materials based on 4d and 5d transition metals. *Chem. Soc. Rev.* **2011**, *40*, 3213–3238. [[CrossRef](#)] [[PubMed](#)]
7. Clemente-Juan, J.M.; Coronado, E.; Gaita-Arino, A. Magnetic polyoxometalates: From molecular magnetism to molecular spintronics and quantum computing. *Chem. Soc. Rev.* **2012**, *41*, 7464–7478. [[CrossRef](#)] [[PubMed](#)]
8. Caneschi, A.; Gatteschi, D.; Totti, F. Molecular magnets and surfaces: A promising marriage. A DFT insight. *Coord. Chem. Rev.* **2015**, *289–290*, 357–378. [[CrossRef](#)]
9. Liu, K.; Shi, W.; Cheng, P. Toward heterometallic single-molecule magnets: Synthetic strategy, structures and properties of 3d–4f discrete complexes. *Coord. Chem. Rev.* **2015**, *289–290*, 74–122. [[CrossRef](#)]
10. Rams, M.; Peresyphkina, E.V.; Mironov, V.S.; Wernsdorfer, W.; Vostrikova, K.E. Magnetic relaxation of 1D coordination polymers (x)₂[Mn(acacen)Fe(CN)₆], X = Ph₄P⁺, Et₄N⁺. *Inorg. Chem.* **2014**, *53*, 10291–10300. [[CrossRef](#)] [[PubMed](#)]
11. MasPOCH, D.; Ruiz-Molina, D.; Veciana, J. Magnetic nanoporous coordination polymers. *J. Mater. Chem.* **2004**, *14*, 2713–2723. [[CrossRef](#)]
12. MasPOCH, D.; Ruiz-Molina, D.; Veciana, J. Old materials with new tricks: Multifunctional open-framework materials. *Chem. Soc. Rev.* **2007**, *36*, 770–818. [[CrossRef](#)] [[PubMed](#)]

13. Chorazy, S.; Nakabayashi, K.; Arczynski, M.; Pelka, R.; Ohkoshi, S.; Sieklucka, B. Multifunctionality in bimetallic $\text{Ln}^{\text{III}}[\text{W}^{\text{V}}(\text{CN})_8]^{3-}$ ($\text{Ln} = \text{Gd}, \text{Nd}$) coordination helices: Optical activity, luminescence, and magnetic coupling. *Chem. Eur. J.* **2014**, *20*, 7144–7159. [[CrossRef](#)] [[PubMed](#)]
14. Pedersen, K.S.; Sigrist, M.; Sørensen, M.A.; Barra, A.-L.; Weyhermüller, T.; Piligkos, S.; Thuesen, C.A.; Vinum, M.G.; Mutka, H.; Weihe, H.; *et al.* [ReF_6] $^{2-}$: A robust module for the design of molecule-based magnetic materials. *Angew. Chem.* **2014**, *126*, 1375–1378. [[CrossRef](#)]
15. Shurdha, E.; Lapidus, S.H.; Stephens, P.W.; Moore, C.E.; Rheingold, A.L.; Miller, J.S. Extended network thiocyanate- and tetracyanoethanide-based first-row transition metal complexes. *Inorg. Chem.* **2012**, *51*, 9655–9665. [[CrossRef](#)] [[PubMed](#)]
16. Massoud, S.S.; Quan, L.L.; Gatterer, K.; Albering, J.H.; Fischer, R.C.; Mautner, F.A. Structural characterization of five-coordinate copper(II), nickel(II), and cobalt(II) thiocyanato complexes derived from bis(2-(3,5-dimethyl-1-pyrazolyl)ethyl)amine. *Polyhedron* **2012**, *31*, 601–606. [[CrossRef](#)]
17. Małecki, J.G.; Groń, T.; Duda, H. Structural, spectroscopic and magnetic properties of thiocyanate complexes of Mn(II), Ni(II) and Cu(II) with the 1-methylimidazole ligand. *Polyhedron* **2012**, *36*, 56–68. [[CrossRef](#)]
18. Wriedt, M.; Jeß, I.; Näther, C. Synthesis, crystal structure, and thermal and magnetic properties of new transition metal-pyrazine coordination polymers. *Eur. J. Inorg. Chem.* **2009**, 1406–1413. [[CrossRef](#)]
19. Létard, J.-F.; Asthana, S.; Shepherd, H.J.; Guionneau, P.; Goeta, A.E.; Suemura, N.; Ishikawa, R.; Kaizaki, S. Photomagnetism of a sym-cis-dithiocyanato iron(II) complex with a tetradentate n,n' -bis(2-pyridylmethyl)1,2-ethanediamine ligand. *Chem. Eur. J.* **2012**, *18*, 5924–5934. [[CrossRef](#)] [[PubMed](#)]
20. González, R.; Acosta, A.; Chiozzone, R.; Kremer, C.; Armentano, D.; De Munno, G.; Julve, M.; Lloret, F.; Faus, J. New family of thiocyanate-bridged Re(IV)-SCN-M(II) ($\text{M} = \text{Ni}, \text{Co}, \text{Fe}, \text{and Mn}$) heterobimetallic compounds: Synthesis, crystal structure, and magnetic properties. *Inorg. Chem.* **2012**, *51*, 5737–5747. [[CrossRef](#)] [[PubMed](#)]
21. Palion-Gazda, J.; Machura, B.; Lloret, F.; Julve, M. Ferromagnetic coupling through the end-to-end thiocyanate bridge in cobalt(II) and nickel(II) chains. *Cryst. Growth Des.* **2015**, *15*, 2380–2388. [[CrossRef](#)]
22. Werner, J.; Rams, M.; Tomkowicz, Z.; Runčevski, T.; Dinnebier, R.E.; Suckert, S.; Näther, C. Thermodynamically metastable thiocyanato coordination polymer that shows slow relaxations of the magnetization. *Inorg. Chem.* **2015**, *54*, 2893–2901. [[CrossRef](#)] [[PubMed](#)]
23. Mautner, F.; Louka, F.; Gallo, A.; Albering, J.; Saber, M.; Burham, N.; Massoud, S. Thiocyanato-copper(II) complexes derived from a tridentate amine ligand and from alanine. *Transit. Met. Chem.* **2010**, *35*, 613–619. [[CrossRef](#)]
24. Werner, J.; Runčevski, T.; Dinnebier, R.; Ebbinghaus, S.G.; Suckert, S.; Näther, C. Thiocyanato coordination polymers with isomeric coordination networks—Synthesis, structures, and magnetic properties. *Eur. J. Inorg. Chem.* **2015**, *20*, 3236–3245. [[CrossRef](#)]
25. Massoud, S.S.; Dubin, M.; Guilbeau, A.E.; Spell, M.; Vicente, R.; Wilfling, P.; Fischer, R.C.; Mautner, F.A. Azido- and thiocyanato-cobalt(II) complexes based pyrazole ligands. *Polyhedron* **2014**, *78*, 135–140. [[CrossRef](#)]
26. Machura, B.; Świtlicka, A.; Zwoliński, P.; Mroziński, J.; Kalińska, B.; Kruszynski, R. Novel bimetallic thiocyanate-bridged Cu(II)–Hg(II) compounds—Synthesis, x-ray studies and magnetic properties. *J. Solid State Chem.* **2013**, *197*, 218–227. [[CrossRef](#)]
27. Machura, B.; Świtlicka, A.; Mroziński, J.; Kalińska, B.; Kruszynski, R. Structural diversity and magnetic properties of thiocyanate copper(II) complexes. *Polyhedron* **2013**, *52*, 1276–1286. [[CrossRef](#)]
28. Massoud, S.S.; Guilbeau, A.E.; Luong, H.T.; Vicente, R.; Albering, J.H.; Fischer, R.C.; Mautner, F.A. Mononuclear, dinuclear and polymeric 1d thiocyanato- and dicyanamido-copper(II) complexes based on tridentate coligands. *Polyhedron* **2013**, *54*, 26–33. [[CrossRef](#)]
29. Werner, J.; Tomkowicz, Z.; Reinert, T.; Näther, C. Synthesis, structure, and properties of coordination polymers with layered transition-metal thiocyanato networks. *Eur. J. Inorg. Chem.* **2015**, *2015*, 3066–3075. [[CrossRef](#)]
30. Wöhlert, S.; Runčevski, T.; Dinnebier, R.E.; Ebbinghaus, S.G.; Näther, C. Synthesis, structures, polymorphism, and magnetic properties of transition metal thiocyanato coordination compounds. *Cryst. Growth Des.* **2014**, *14*, 1902–1913. [[CrossRef](#)]
31. Mousavi, M.; Bereau, V.; Duhayon, C.; Guionneau, P.; Sutter, J.-P. First magnets based on thiocyanato-bridges. *Chem. Commun.* **2012**, *48*, 10028–10030. [[CrossRef](#)] [[PubMed](#)]

32. Mautner, F.A.; Scherzer, M.; Berger, C.; Fischer, R.C.; Vicente, R.; Massoud, S.S. Synthesis and characterization of five new thiocyanato- and cyanato-metal(II) complexes with 4-azidopyridine as co-ligand. *Polyhedron* **2015**, *85*, 20–26. [[CrossRef](#)]
33. Uhrecký, R.; Ondrejkočková, I.; Lacková, D.; Fáberová, Z.; Mroziński, J.; Kalińska, B.; Padělková, Z.; Koman, M. New thiocyanato iron(II) complex with 3,5-bis(3-pyridyl)-1,2,4-thiadiazole: Synthesis, structure, magnetic and spectral properties. *Inorg. Chim. Acta* **2014**, *414*, 33–38. [[CrossRef](#)]
34. Banerjee, S.; Wu, B.; Lassahn, P.-G.; Janiak, C.; Ghosh, A. Synthesis, structure and bonding of cadmium(II) thiocyanate systems featuring nitrogen based ligands of different denticity. *Inorg. Chim. Acta* **2005**, *358*, 535–544. [[CrossRef](#)]
35. Werner, J.; Rams, M.; Tomkowicz, Z.; Näther, C. A Co(II) thiocyanato coordination polymer with 4-(3-phenylpropyl)pyridine: The influence of the co-ligand on the magnetic properties. *Dalton Trans.* **2014**, *43*, 17333–17342. [[CrossRef](#)] [[PubMed](#)]
36. Boeckmann, J.; Wriedt, M.; Näther, C. Metamagnetism and single-chain magnetic behavior in a homospin 1d iron(II) coordination polymer. *Chem. Eur. J.* **2012**, *18*, 5284–5289. [[CrossRef](#)] [[PubMed](#)]
37. Wöhlert, S.; Ruschewitz, U.; Näther, C. Metamagnetism and slow relaxation of the magnetization in the 2d coordination polymer: $[\text{Co}(\text{NCS})_2(1,2\text{-bis}(4\text{-pyridyl})\text{ethylene})]_n$. *Cryst. Growth Des.* **2012**, *12*, 2715–2718. [[CrossRef](#)]
38. Näther, C.; Wöhlert, S.; Boeckmann, J.; Wriedt, M.; Jeß, I. A rational route to coordination polymers with condensed networks and cooperative magnetic properties. *Z. Anorg. Allg. Chem.* **2013**, *639*, 2696–2714. [[CrossRef](#)]
39. Boeckmann, J.; Näther, C. Metamagnetism and long range ordering in $\mu\text{-}1,3$ bridging transition metal thiocyanato coordination polymers. *Polyhedron* **2012**, *31*, 587–595. [[CrossRef](#)]
40. Werner, J.; Neumann, T.; Näther, C. Synthesis, structures, and properties of transition metal thiocyanato coordination compounds with 4-(4-chlorobenzyl)pyridine as ligand. *Z. Anorg. Allg. Chem.* **2014**, *640*, 2839–2846. [[CrossRef](#)]
41. Wöhlert, S.; Peters, L.; Näther, C. Synthesis, structures and magnetic properties of Fe(II) and Co(II) thiocyanato coordination compounds: On the importance of the diamagnetic counterparts for structure determination. *Dalton Trans.* **2013**, *42*, 10746–10758. [[CrossRef](#)] [[PubMed](#)]
42. Wöhlert, S.; Näther, C. Structures and magnetic properties of nickel thiocyanato coordination compounds with 2-chloropyrazine as a neutral coligand. *Eur. J. Inorg. Chem.* **2013**, *2013*, 2528–2537. [[CrossRef](#)]
43. Wöhlert, S.; Wriedt, M.; Fic, T.; Tomkowicz, Z.; Haase, W.; Näther, C. Synthesis, crystal structure and magnetic properties of the coordination polymer $[\text{Fe}(\text{NCS})_2(1,2\text{-bis}(4\text{-pyridyl})\text{-ethylene})]_n$ showing a two step metamagnetic transition. *Inorg. Chem.* **2013**, *52*, 1061–1068. [[CrossRef](#)] [[PubMed](#)]
44. Wöhlert, S.; Tomkowicz, Z.; Rams, M.; Ebbinghaus, S.G.; Fink, L.; Schmidt, M.U.; Näther, C. Influence of the co-ligand on the magnetic and relaxation properties of layered Co(II) thiocyanato coordination polymers. *Inorg. Chem.* **2014**, *53*, 8298–8310. [[CrossRef](#)] [[PubMed](#)]
45. Wöhlert, S.; Boeckmann, J.; Wriedt, M.; Näther, C. Coexistence of metamagnetism and slow relaxation of magnetization in a cobalt thiocyanate 2d coordination network. *Angew. Chem. Int. Ed.* **2011**, *50*, 6920–6923. [[CrossRef](#)] [[PubMed](#)]
46. Werner, J.; Tomkowicz, Z.; Rams, M.; Ebbinghaus, S.G.; Neumann, T.; Näther, C. Synthesis, structure and properties of $[\text{Co}(\text{NCS})_2(4\text{-}(4\text{-chlorobenzyl})\text{pyridine})_2]_n$, that shows slow magnetic relaxations and a metamagnetic transition. *Dalton Trans.* **2015**, *44*, 14149–14158. [[CrossRef](#)] [[PubMed](#)]
47. Wöhlert, S.; Fic, T.; Tomkowicz, Z.; Ebbinghaus, S.G.; Rams, M.; Haase, W.; Näther, C. Structural and magnetic studies of a new Co(II) thiocyanato coordination polymer showing slow magnetic relaxations and a metamagnetic transition. *Inorg. Chem.* **2013**, *52*, 12947–12957. [[CrossRef](#)] [[PubMed](#)]
48. Maroszová, J.; Moncol, J.; Padělková, Z.; Sillanpää, R.; Lis, T.; Koman, M. Self-assembled hydrogen-bonded coordination networks in two copper(II) carboxylates with 4-pyridylmethanol. *Cent. Eur. J. Chem.* **2011**, *9*, 453–459. [[CrossRef](#)]
49. Moncol, J.; Mudra, M.; Lonneck, P.; Koman, M.; Melnik, M. Hydrogen-bonded coordination network in crystal structures of $[\text{Cu}(3\text{-PM})_4\text{Cl}_2]$ and $[\text{Cu}(4\text{-PM})_4\text{Cl}]\text{Cl}$, (PM = pyridylmethanol). *J. Chem. Crystallogr.* **2004**, *34*, 423–431. [[CrossRef](#)]

50. Moncol, J.; Kalinakova, B.; Svorec, J.; Kleinova, M.; Koman, M.; Hudecova, D.; Melnik, M.; Mazur, M.; Valko, M. Spectral properties and bio-activity of copper(II) clofibrates, part III: Crystal structure of $\text{Cu}(\text{clofibrate})_2(2\text{-pyridylmethanol})_2$, $\text{Cu}(\text{clofibrate})_2(4\text{-pyridylmethanol})_2(\text{H}_2\text{O})$ dihydrate, and $\text{Cu}_2(\text{clofibrate})_4(\text{n,n-diethylnicotinamide})_2$. *Inorg. Chim. Acta* **2004**, *357*, 3211–3222. [[CrossRef](#)]
51. Stamatatos, T.C.; Foguet-Albiol, D.; Perlepes, S.P.; Raptopoulou, C.P.; Terzis, A.; Patrickios, C.S.; Christou, G.; Tasiopoulos, A.J. 4-(hydroxymethyl)pyridine and pyrimidine in manganese benzoate chemistry: Preparation and characterization of hexanuclear clusters featuring the core. *Polyhedron* **2006**, *25*, 1737–1746. [[CrossRef](#)]
52. Goher, M.A.S.; Mautner, F.A.; Gatterer, K.; Abu-Youssef, M.A.M.; Badr, A.M.A.; Sodin, B.; Gspan, C. Four $[\text{Cd}(\text{L})_2(\text{N}_3)_2]_n$ 1d systems with different azide bridging sequences: Synthesis, spectral and structural characterization. *J. Mol. Struct.* **2008**, *876*, 199–205. [[CrossRef](#)]
53. Werner, J.; Näther, C. Synthesis, crystal structures and properties of $\text{Ni}(\text{NCS})_2\text{-}4\text{-(hydroxymethyl)pyridine}$ coordination compounds. *Polyhedron* **2015**, *98*, 96–104. [[CrossRef](#)]
54. Uçar, İ.; Bulut, İ.; Bulut, A.; Karadağ, A. Polymeric and monomeric dipicolinate complexes with 4-hydroxymethyl pyridine: Spectral, structural, thermal and electrochemical characterization. *Struct. Chem.* **2009**, *20*, 825–838. [[CrossRef](#)]
55. Sheldrick, G.M. A short history of SHELX. *Acta Crystallogr. Sect. A* **2008**, *64*, 112–122. [[CrossRef](#)] [[PubMed](#)]
56. Bruker, A.X.S. *Topas*; Version 5.0; Bruker: Karlsruhe, Germany, 2014.
57. Coelho, A. Whole-profile structure solution from powder diffraction data using simulated annealing. *J. Appl. Cryst.* **2000**, *33*, 899–908. [[CrossRef](#)]



© 2016 by the authors; licensee MDPI, Basel, Switzerland. This article is an open access article distributed under the terms and conditions of the Creative Commons by Attribution (CC-BY) license (<http://creativecommons.org/licenses/by/4.0/>).